FINAL REPORT

Effect of molecular structure variation on the kinetics and thermodynamics of inclusion in biocompatible macrocycles

Macrocyclic compounds are widely used building blocks in supramolecular chemistry and nanotechnology. Their inclusion complex formation has a continuously expanding range of applications, for example in the drug delivery, cellular imaging, catalysis, and sensing. In this project, we focused on the noncovalent binding to two types of water-soluble biocompatible macrocycles, cucurbit[n]urils (CBn) and 4-sulfonatocalix[n]arenes (SCXn). Figure 1 displays the formulas of these host compounds. Our systematic studies revealed the kinetics and thermodynamics of the association with the former class of cavitands, whereas the later family of compounds were used to create complexes, supramolecular micelles, nanoparticles, and stimuli-responsive systems. Our investigations were extended to the effects of amino acids or anionic pyrene derivatives on the self-assembly of 1-tetradecyl-3-methylimidazolium bromide in water. In addition, we developed fluorescence probes applicable to confocal microscopic imaging of live cells and to the monitoring of calcium in hard water.

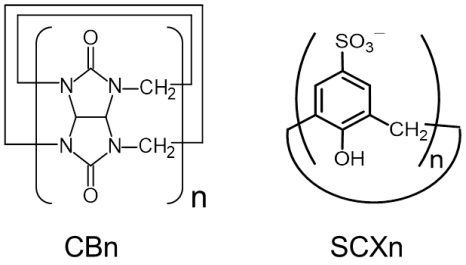

Figure 1 Chemical structures of the host compounds

1. Kinetics and thermodynamics of the reversible binding to cucurbit[n]urils

Because of the great potential of the CBn homologue composed of 7 glycoluril units linked by a pair of methylene groups in the stabilization and delivery of drugs, we revealed the effect of molecular structure variation on the kinetics of entry into and exit from cucurbit[7]uril (CB7) cavity. Protoberberine alkaloids (Figure 2), which are the active components of the traditional Chinese herbal medicines and exhibit diverse biological and

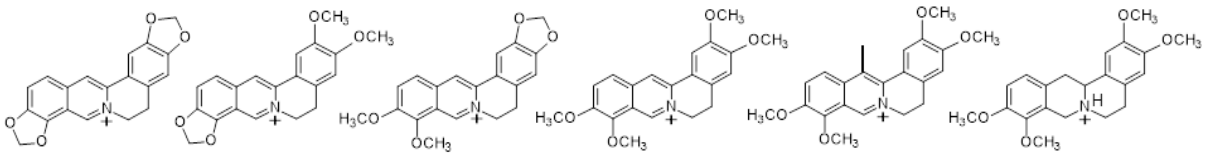

Figure 2 Structural formulas of the guest alkaloids

pharmaceutical effects, were chosen as guest compounds. Our results demonstrate that the formation and dissociation of the highly stable alkaloid–CB7 1:1 complexes are sterically hindered and possess substantial energy barriers, which depend on the relative size of the guest and the portal of the macrocycle. In the thermodynamically most favourable complex structure, the isoquinoline part of the studied alkaloids is encompassed by the host. The introduction of bulky substituents into this moiety can essentially alter the dynamics of encapsulation. The sterically less demanding part of the guest passes through the narrow opening of CB7 and afterwards, the most stable position is reached. Despite the same thermodynamic parameters of berberine and palmatine inclusion, the latter compound was encapsulated in and set free from CB7 much slower due to the more substantial steric hindrance. The most rapid entry into CB7 and the most exothermic binding were found for epiberberine and coptisine, the alkaloids substituted with the less spacious dioxole ring on their isoquinoline moiety.

We also unravelled how the introduction of hydrogen atoms or a methyl substituent into a pharmacologically active natural alkaloid, palmatine (P^+) influenced the rate constants of the embedment into and release from CB7. Both the hydrogenated form, the protonated tetrahydropalmatine (THP^+) and the methylated derivative, dehydrocorydaline (DHC^+) produced 1:1 complexes with CB7 in enthalpy controlled processes without any detectable intermediates. The tight entrance of the host compound imposed substantial steric barrier for encapsulation making the ingression several orders of magnitude slower than diffusion. Despite the ~6 kJ mol^{-1} lower activation enthalpy, the rate constant of THP^+ entry into CB7 was about 44-fold smaller at 298 K than that of DHC^+, as a consequence of the considerably negative activation entropy of the former binding. The egression rates of the two studied alkaloids differed to a much lesser extent because the lower energy barrier of THP^+ release was almost compensated by the unfavourable activation entropy. In comparison with the kinetics of the reversible confinement of the palmatine parent compound, the presence of the methyl substituent on the aromatic heterocyclic ring in DHC^+ barely modified the rate constant of entry into CB7 but caused about 10-fold increase in the dissociation rate at 298 K. A tightly bound transition state is produced in the course of entry into CB7 when the guest contained a nonaromatic heterocycle with localized charge, such as THP^+. On the other hand, host–guest interaction was weak in the transition state when the positive charge of the nitrogen was distributed throughout the aromatic rings of the guests like in P^+ and DHC^+.

The knowledge of the association ability of CBn macrocycles with metal cations is essential for their application in stimuli-responsive systems, drug delivery, assays, and

biologically relevant buffered media. Therefore, we revealed in collaboration with German scientists how the size and charge of 19 inorganic cations affect their affinity to CBn homologues possessing 5, 6, 7, or 8 glycoluril units. The binding selectivity lessened with the growth of macrocycle size. CBn hosts proved to be similarly efficient metal ion receptors as 4-sulfonatocalix[4]arene and they outperformed 18-crown-6 crown ether. The binding constants usually increased for larger and less strongly hydrated alkali and alkaline earth ions but a bell-shaped ion radius dependence was found for the alkali ion complexations with cucurbit[5]uril. In the case of this smallest and most rigid cavitand, the ideal size matching is important for strong confinement. Rb^+ and Cs^+ are too large to penetrate into the carbonyl portal region of CB5, where the dipolar interaction with the oxygen lone pairs is most effective. H_3O^+ and NH_4^+ showed weaker binding than the similarly sized monovalent metal ions because their efficient hydrogen bonding with water hindered the ion–dipole interactions with the carbonyl laced entrance of CBn. Our results demonstrate that the apparent binding constants and thermodynamic parameters available in the literature for guest–CBn complexation in the presence of buffers or salts are incorrect in absolute terms because the competitive binding of inorganic cations significantly alters the obtained values.

Selective measurement of the overall rate constant of inclusion complex dissociation shed light on the subtle kinetic details of the salt-promoted guest release from the cavity of CB7. Two contrasting mechanisms were identified. The symmetric dicationic 2,7-dimethyldiazapyrenium showed a cation-independent complex dissociation coupled to deceleration of the ingression in the presence of alkali and alkaline earth cations (M^{n+}) due to competitive formation of CB7–M^{n+} complexes. In contrast, a more complicated, unprecedented kinetic behaviour was observed for the ingression and egression of the monocationic and non-symmetric berberine (B^+). The formation of B^+–CB7–M^{n+} ternary complex was unambiguously identified. B^+ dissociated faster from the ternary complex than from B^+–CB7 but the rate enhancement showed less than twofold change with M^{n+}. In contrast, a more than two orders of magnitude increase was found in the equilibrium constants of M^{n+} binding to B^+–CB7 inclusion complex with the size and charge of cations. Remarkably different, new kinetic features appeared at high K^+ and Ba^{2+} concentrations when B^+–CB7–M^{n+} outweighed B^+–CB7. Under these conditions, the large K^+ and Ba^{2+} cations also promoted B^+ expulsion from the ternary complex in a bimolecular process. The motion of M^{n+} toward ternary complex B^+–CB7–M^{n+} is probably coupled with the displacement of B^+ from the host cavity and the production of M^{n+}–CB7– M^{n+} complex. This reaction is the supramolecular analogue of the S_E2 type of electrophilic substitution in

organic chemistry. In such reactions, the formation of the new bond and the breaking of the old bond take place simultaneously via a single transition state. The optimal size of M^{n+} is important, because cations with radius of approximately 100 pm or smaller are unable to participate in such a process, whereas organic cations are too big and usually have delocalised charge, which makes this type of transformations unfavourable. The bimolecular B^+ removal by Ba^{2+} has an approximately 20-fold larger rate constant than by K^+. Because of its double positive charge, the former ion more efficiently promotes the expulsion of B^+. Changing the anion modified the kinetic traces only to a negligible extent indicating that ionic strength does not influence B^+ release.

During the study of the inclusion complex formation of quaternary benzo[c]phenanthridine plant alkaloids, nitidine, sanguinarine, and chelerythrine (Figure 3),

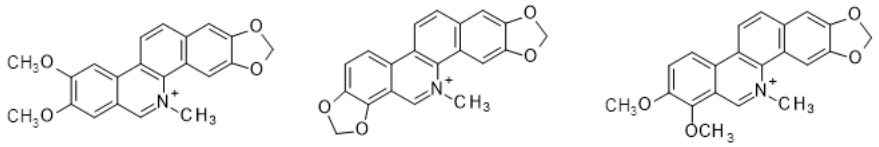

Figure 3 Structural formulas of the quaternary benzo[c]phenanthridine alkaloids

we found that the unexpected results originated from dimer formation in water. The increase of alkaloid concentration brought about moderate changes in the absorption spectra, while the fluorescence properties altered only in the case of nitidine. The lack of fluorescence from sanguinarine and chelerythrine dimers was explained by their rapid dissociation to singlet-excited and ground-state monomers. Enthalpy-controlled self-binding occurred and the variation of the association enthalpy was substantially compensated by the unfavourable entropic term. Nitidine dimerization was the most exothermic and the equilibrium constant of this process exceeded by a factor of ~5 the corresponding values of the other two alkaloids. The results of quantum chemical calculations agreed well with the experimental data and provided information on the structural features of the dimers.

In collaboration with German researchers, time-resolved methods were introduced which allow for convenient determination of rate constants of spectroscopically silent or even almost insoluble guests with the macrocyclic cucurbit[n]uril family and human serum albumin (HSA) protein as representative hosts. The alteration of the fluorescence properties of 5 indicator dyes upon complexation was used to monitor the expulsion of the indicator dye by a guest (kinetic indicator displacement assay, *kin*IDA) or the replacement of a guest by an indicator dye in the host in real time. The latter kinetic guest displacement assay (*kin*GDA)

method could provide rate constants even for the reversible binding of barely soluble, nonfluorescent estradiol because of the substantial solubility enhancement upon host-guest binding. If the pseudo-first order rate constant of guest ingression was much larger than that of the indicator dye, the rate constant of guest egression could be selectively measured. More than 5 orders of magnitude slower exit was found from CB7 than from the bulkier cucurbit[8]uril (CB8) for 1-adamantanol, whose dimensions matched well the size of the CB7 cavity. In contrast, the rate constant of nortestosterone ingression diminished to a larger extent than the rate constant of its egression when CB8 host was replaced by CB7. We demonstrated the lack of correlation between the Gibb's free energy of host-guest association and the Gibb's free energy of activation of complexation and decomplexation.

An alternative method, the kinetic simultaneous analyte indicator binding assay (*kin*SBA) was also developed for the accurate determination of the rate constants of entry into and exit from cavitands. In *kin*SBA, a solution of a host is rapidly mixed with a solution of an indicator dye, whose kinetic parameters are already known and of spectroscopically silent guest, whose kinetic rate constants are to be determined. Upon mixing, the temporal change of a spectroscopic signal, indicative of the time-dependent ratio of free and bound indicator dye, are monitored. This method offers several advantages. (i) Very low host concentration is sufficient for the measurement, which is particularly important for barely soluble, expensive, or sparingly available hosts. (ii) The use of dilute host solution reduces the risk of the undesirable interference of ternary complexation. (iii) The system of differential equations describing the temporal characteristics of the detected signal can be solved analytically if the guest and dye are present in a large (at least 10-fold) excess compared to the host. This simplifies the analysis of the experimental data to a nonlinear least-squares fit. (iv) Moreover, *kin*SBA can serve as a sensitive rapid test to screen the time required for the establishment of the host-guest binding equilibrium. When thermodynamic quantities or association constants are measured by titrations, it should always be verified that the chemical equilibrium is reached after each addition to avoid substantial systematic error in the obtained parameters. (v) The contributions of ingression and egression to the kinetic traces are more separated in time than in other kinetic assays facilitating more precise rate constant determination. (vi) The observed signal shape provides immediate qualitative insight into the relationship among the rate constants. The *kin*SBA method was tested with computer simulations and experimentally using various host-guest pairs.

The experience acquired in the field of the CBn inclusion complexes was used in the study of the stability of the various regions of human ileal bile acid-binding protein in

collaboration with several Hungarian research groups. Fluorescence spectroscopic measurements contributed to the deeper understanding of the internal dynamics of this protein, which has a key role in the intracellular transport and metabolic targeting of bile salts. The intensity and the location of the maximum of the fluorescence exhibited marked temperature dependence. These data provided information on the temperature-induced unfolding of the protein. Most of the fluorescence signal arose from a single buried tryptophan unit.

2. Self-assembly with 4-sulfonatocalix[n]arenes

4-Sulfonatocalix[6]arene-induced associations of various cationic surfactants containing tetradecyl tail were studied in collaboration with French researchers to reveal the impact of the properties of the headgroup on the thermodynamics of the self-assembly to supramolecular micelles and nanoparticles in aqueous solutions at pH 7. When the surfactant contained hydrophilic trimethylammonium, pyridinium, or 1-methylimidazolium headgroup, highly reversible temperature-responsive nanoparticle−supramolecular micelle transformation could be attained at appropriately chosen component mixing ratios and NaCl concentrations. In these cases, the substantial negative molar heat capacity change rendered nanoparticle formation strongly endothermic at low temperature, whereas the assembly to supramolecular micelle was always accompanied by enthalpy gain. The molar heat capacity change became less negative when the charge density and the hydrophilic character of the surfactant headgroup diminished. The association of the more hydrophobic 6-methoxyquinolinium and quinolinium surfactants with 4-sulfonatocalix[6]arene did not lead to supramolecular micelle formation because the self-assembly into nanoparticles was highly exothermic.

We also unravelled how the size of the SCXn macrocycle and the chain length of the substituents of 1-alkyl-6-alkoxy-quinolinium ($m \leq 8$, Fig. 4) ions affect the thermodynamics

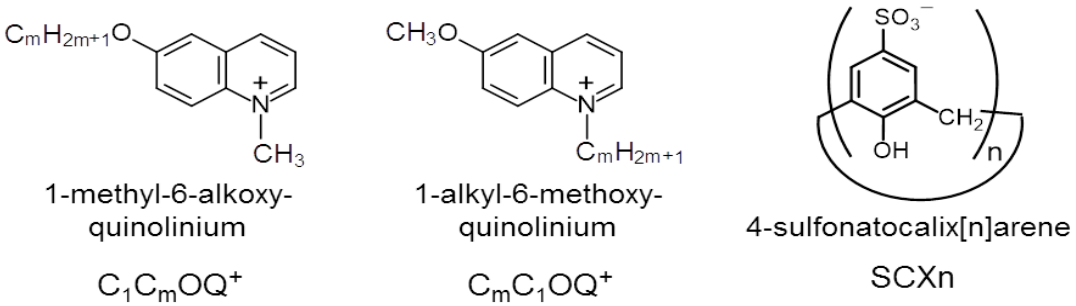

Figure 4 Structural formulas of the components

of 1:1 binding of these compounds. The equilibrium constants of complexation were always larger for the confinement in 4-sulfonatocalix[4]arene (SCX4) than in its 4-sulfonatocalix[6]arene (SCX6) homologue because the better matching between the host and guest sizes allowed more exothermic interaction. The binding affinity diminished with the lengthening of the aliphatic chain of the guests in the case of the association with SCX4, but insignificant change was found for SCX6 complexes. The most substantial change in the enthalpic and entropic contributions to the driving force of complexation occurred when the alkyl chain was linked to the heterocyclic nitrogen ($C_mC_1OQ^+$) and the number of its carbon atoms varied between 1 and 4. NMR spectra showed that the quinolinium ring is always inside SCX4, but the alkyl chain is included only for a short chain length (n up to 4). In contrast, the alkoxy chain of $C_1C_mOQ^+$ (Figure 4) displayed a very weak interaction with the cavity irrespective of the length. Because of the outward orientation from the host, the lengthening of the alkoxy substituent of the quinolinium moiety barely influenced the thermodynamics of inclusion in SCX4. Distinct linear enthalpy−entropy correlations were found for the encapsulation in SCX4 and SCX6.

$C_1C_mOQ^+$ (m = 8, 10, or 12) and $C_mC_1OQ^+$ (m = 10, 12, or 14) self-assembled with SCXn into nanoparticles (NP) in neutral aqueous solutions at 298 K. The size, zeta potential and composition of NP were determined over a large molar mixing ratio range. Isothermal titration calorimetry showed that host-guest binding assisted the formation of negatively charged NPs in exothermic processes. The enthalpy gain in these associations significantly increased with the lengthening of the 1-alkyl group but was insensitive to the size of the SCXn macrocycle. The morphology of NPs was studied by cryogenic transmission electron microscopy. $C_mC_1OQ^+$ organization with SCXn led to spherical NPs without regular inner structure. In contrast, $C_1C_mOQ^+$–SCXn nanoaggregates usually had various shapes and lamellar domains with ~3nm layer thickness. The different orientation of $C_mC_1OQ^+$ and $C_1C_mOQ^+$ in the cavitand was proposed to rationalize the morphological alterations.

SCXn-promoted nanoparticle production was also examined with a cationic polymer in aqueous solutions. Methylimidazolium side groups were grafted via ether linkage to dextran. Dynamic light scattering and zeta potential measurements revealed the mixing ratio ranges in which this polymer created stable nanoparticles with SCXn macrocycles. The size of SCXn and the molecular mass of the polymer barely affected the nanoparticle diameter, but the lowering of the imidazolium degree of substitution substantially diminished the stability of the associates. The pH change from neutral to acidic also unfavourably influenced the self-organization owing mainly to the decrease of the SCXn charge. Cryogenic

transmission electron microscopy images proved the spherical morphology of the nanoproducts in which the stoichiometry of the constituents was always close to the one corresponding to charge compensation. The flexible and positively charged dextran-chains were compacted by the polyanionic SCXn. These macrocycles not only induced self-assembly with methylimidazolium-conjugated dextrans into NPs by supramolecular crosslinking of the polymer chains but also could serve as molecular containers within NPs to encapsulate the biomedically important alkaloid, coralyne. This compound was efficiently embedded by self-assembly in the produced nanoparticles reaching 99% association efficiency.

In collaboration with Japanese scientists, we examined how the encapsulation in the SCXn cavity modifies the electron transfer kinetics of methylviologen at glassy carbon electrode. The electrochemical electron transfer of the inclusion complex was found to be adiabatical and its activation energy was about 70–80% lower than that of free methylviologen.

3. Self-assembly of 1-tetradecyl-3-methylimidazolium bromide in the presence of additives

Self-organization was also observed in the interaction of anionic pyrene derivatives with cationic surfactants bearing a tetradecyl chain (Figure 5). Two types of nanoparticles

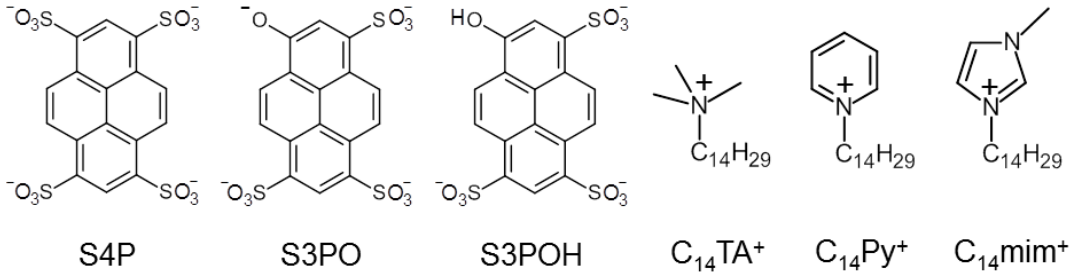

Figure 5 Chemical formulas of the used compounds

were produced depending on the mixing ratio of the components. The self-assembly to negatively charged larger nanoparticles at low surfactant excess was always exothermic, whereas the formation and size diminution of the positive nanoparticles in the presence of larger amounts of surfactants were practically thermoneutral. The alteration of the fluorescence spectrum upon self-organization of the constituents indicated π–π interaction between the pyrene moieties within the nanoparticles. In tetradecyltrimethylammonium bromide solution, 1,3,6,8-pyrenetetrasulfonate (S4P) induced the formation of not only nanoparticles but also mixed micelles composed of supramolecular and conventional amphiphiles. A pH-responsive entropy-controlled transformation of nanoparticles to such

mixed micelles was achieved when 1-methyl-3-tetradecyl-imidazolium cation had more than 19-fold molar excess over 8-hydroxypyrene-1,3,6-trisulfonate (S3POH).

Effect of amino acid addition on the micelle formation of 1-tetradecyl-3-methylimidazolium bromide in aqueous solution was unravelled in cooperation with a Chilean research group. The most substantial critical micelle concentration diminution was observed in the presence of L-tryptophan at pH 12, due to the electrostatic and π–π interactions with the imidazolium headgroup of the surfactant. Always entropy-driven micellization occurred. Both the enthalpy and entropy changes upon association to micelles increased when the pH was raised from 7 to 12. ^{1}H NMR measurements demonstrated that among the used amino acids, L-tryptophan interacts most strongly with the headgroup of the surfactant cation. The knowledge on the surfactant–amino acid interactions significantly contributes to the deeper understanding of the effect of surfactants on the properties of peptides.

4. Development of fluorescent probes

The fluorescent behaviour of carbon nanodots was investigated as a joint project with Japanese and Bulgarian scientists. The effect of preparation methods on the fluorescence characteristics of carbon nanodots was unravelled. The sulphur doped carbon nanodots could be used as nanosensor for rapid and sensitive determination of dissolved calcium ion concentrations and water hardness. The incorporation of sulphur brought about significant shift of the fluorescence maximum to higher energy but did not influence the fluorescence quantum yield.

In cooperation with Croatian scientists, the photophysical and photochemical properties of various N-adamantylphthalimide derivatives were systematically investigated. Among the synthesized compounds, 4-amino-N-adamantylphthalimide proved to be an excellent new fluorescent probe for the confocal microscopic imaging of live cells. This dye had low cytotoxicity, high quantum yield of fluorescence, and could be excited in the near-visible part of the spectrum. The position of its fluorescence maximum and the Stokes shift were well correlated with the $E_T(30)$ solvent polarity parameter. Due to its amphiphilic character, the dye stained artificial membranes in liposomes. Using confocal microscopy on two human cancer cell lines, we showed that the dye stains primarily intracellular lipid droplets. Colocalization experiments with different organelle markers indicated that the additional staining of mitochondrial membranes. The fluorosolvatochromism of the new dye allowed the simultaneous visualization of mitochondria and intracellular lipid droplets in two

separate emission channels. The unique features make the new probe an attractive candidate for the vital staining of cells and tissues involved in lipid storage and intense oxidative metabolism.

The results of this project were published in 18 scientific papers, whose total impact factor is 76.6. These articles have already received 102 independent citations despite the short time passed since their publication. The OTKA/NKFIH grant significantly contributed to the successful collaborations with French, German, Japanese, Croatian, Bulgarian, and Chilean researchers.